

An Improved Bayesian Framework for Quadrature of Constrained Integrands

Henry Chai¹ Roman Garnett¹

Abstract

Quadrature is the problem of estimating intractable integrals, a problem that arises in many Bayesian machine learning settings. We present an improved Bayesian framework for estimating intractable integrals of specific kinds of constrained integrands. We derive the necessary approximation scheme for a specific and especially useful instantiation of this framework: the use of a log transformation to model non-negative integrands. We also propose a novel method for optimizing the hyperparameters associated with this framework; we optimize the hyperparameters in the original space of the integrand as opposed to in the transformed space, resulting in a model that better explains the actual data. Experiments on both synthetic and real-world data demonstrate that the proposed framework achieves more-accurate estimates using less wall-clock time than previously proposed Bayesian quadrature procedures for non-negative integrands.

1. Introduction

Model selection is a fundamental problem that naturally arises in the course of scientific inquiry: given a set of candidate models, how does one determine which model best explains an observed data set? Performing model selection in a Bayesian manner requires the computation of model evidences; these are integrals of the form $Z = \int f(D | x) \pi(x) dx$ where D is the observed data set, x is a set of hyperparameters that govern the model, $f(D | x)$ is a likelihood and $\pi(x)$ is a prior. Integrals of this type are common when using Bayesian machine learning methods, arising when one needs to marginalize over hyperparameters, calculate predictive distributions, or compute marginal likelihoods. Note that the integrand in these types of integrals is known *a priori* to be non-negative as it is the

¹Department of Computer Science and Engineering, Washington University in St. Louis, St. Louis, MO, USA. Correspondence to: Henry Chai <hchai@wustl.edu>.

Work submitted to the International Conference on Machine Learning (ICML), currently under review. Copyright 2018 by the author(s).

product of probability densities. Unfortunately, these integrals are generally computationally intractable and thus must be approximated.

Many commonly used techniques to estimate such integrals rely on Monte Carlo estimators (Neal, 2001; Meng & Wong, 1996; Skilling, 2004). These techniques are agnostic to prior information about the integrand, such as non-negativity, and also converge slowly in terms of the number of required samples of the integrand, making them ill-suited for settings where the integrand is expensive. One alternative to these techniques is Bayesian quadrature (BQ) (Diaconis, 1988; O'Hagan, 1991; Rasmussen & Ghahramani, 2003), which maintains a probabilistic belief on the integrand that can be conditioned on observations to arrive at a distribution over the value of the integral. This belief allows BQ to exploit information-theoretic principles to actively select informative sample locations, increasing sample efficiency.

Recent work by Gunter et al. (2014) improved upon the speed and accuracy of the standard BQ algorithm (SBQ) (Rasmussen & Ghahramani, 2003) by incorporating non-negativity information about the integrand in model-selection problems. Their method models the square root of the integrand instead of the integrand itself; “undoing” this transformation softly incorporates the non-negativity constraint. While previous work (Gunter et al., 2014; Osborne et al., 2012) has shown that specific algorithms can outperform Monte Carlo based methods and SBQ in a variety of settings where the integral is non-negative, a general framework for performing quadrature has never been offered.

Our contribution is to define a Bayesian framework for quadrature (and indeed a wide variety of inference tasks) involving a broader class of constrained functions. We also develop an instantiation of this framework for the important case of non-negative integrands that addresses some shortcomings of previous quadrature work. Specifically, our instantiation allows for estimating integrals of integrands with wider dynamic ranges than the method in (Gunter et al., 2014) and does not require conditioning on randomly-sampled candidate points as in (Osborne et al., 2012). Lastly, we develop a novel procedure for this framework whereby the associated hyperparameters are set by maximizing the marginal likelihood of true observations of the integrand. All previous work that used a transformation to exploit

a priori information fit hyperparameters by maximizing the marginal likelihood of transformed observations. We demonstrate that doing so can lead to undesirable behavior and that our procedure gives a better-behaved model. We conduct experiments on synthetic data and a real-world data set from the realm of astrophysics. The results show that our instantiation of the proposed framework, along with the novel hyperparameter optimization method, outperforms previous BQ algorithms.

2. Bayesian Quadrature

Let

$$\int f(x)\pi(x) dx = Z$$

be an intractable integral; for notational simplicity, all derivations that follow will be written as if $x \in \mathbb{R}$, but note that all results extend to $x \in \mathbb{R}^d$. SBQ operates by placing a Gaussian process (GP) prior on the function f . GPs can be thought of as probability distributions over functions, where the joint distribution of any finite number of function values is multivariate normal. GPs are parametrized by a mean function $m(x)$ and a covariance function $K(x, x')$. Given a set of observations at locations $x_D = \{x_1, \dots, x_n\}$ with corresponding values $f(x_D)$, a GP prior can be conditioned on these observations to arrive at a posterior GP with mean $m_D(x) = m(x) + K(x, x_D)K(x_D, x_D)^{-1}(f(x_D) - m(x_D))$ and covariance $K_D(x, x') = K(x, x') - K(x, x_D)K(x_D, x_D)^{-1}K(x_D, x')$. For a full overview of GPs, see (Rasmussen & Williams, 2006).

If one has a GP belief on the integrand of an integral, then the posterior mean and variance of the integral's value can be derived using the fact that GPs are closed under the evaluation of linear functionals such as integration (Rasmussen & Ghahramani, 2003). Specifically, if $f \sim \mathcal{GP}(m, K)$, then:

$$\begin{aligned} Z &= \int f(x)\pi(x) dx \\ &\sim \mathcal{N}\left(\int m(x)\pi(x) dx, \iint K(x, x')\pi(x)\pi(x') dx dx'\right). \end{aligned} \quad (1)$$

Warped sequential active Bayesian integration (WSABI) (Gunter et al., 2014) builds off of the SBQ algorithm and incorporates non-negativity information by modeling the square root of the integrand. Let $g(x) = \sqrt{2(f(x) - \alpha)}$, so $f(x) = \alpha + g(x)^2/2$ for some small positive constant α . WSABI places a GP prior on g and conditions this prior on observations to arrive at a posterior, much like SBQ. However, when calculating a belief on Z , the key property of closure of GPs under linear functionals is not available using this method because the marginal distribution of any $f(x)$ is a non-central χ^2 distribution. Thus, WSABI approximates the posterior as a GP. Gunter et al. (2014) propose two approximation schemes: linearization, which uses a first-order Taylor expansion around the posterior mean of the GP

on $g(x)$, and moment-matching, which calculates the mean and covariance of the true posterior distribution and defines a GP with these values.

Having a probabilistic belief on the integrand allows one to use information-theoretic principles to select samples, thereby increasing sample efficiency. Whereas Monte Carlo based quadrature techniques are limited to sampling from specific distributions, model-based quadrature methods can select sample locations iteratively to optimize some relevant objective: in WSABI, the samples are chosen via uncertainty sampling, which greedily minimizes the entropy of the integrand, whereas Osborne et al. (2012) chose samples so as to minimize the expected entropy of the integral Z .

3. A Framework for Inference on Constrained Functions

WSABI and its predecessor, the algorithm described by Osborne et al. (2012), can be viewed as instantiations of following general framework for inferring affine transformations of constrained functions where the constraint can be described as a warping of \mathbb{R} , with the caveat that WSABI and its predecessor use a different hyperparameter optimization methodology. Let $Z = L[f]$ be a quantity of interest for some function f and some linear functional L .

1. Determine a warping function ξ that maps from \mathbb{R} to the range of f . Let $g(x) = \xi^{-1}(f(x))$. Place a GP prior on $g \sim \mathcal{GP}(\mu, \Sigma)$.
2. Calculate the mean and variance of the resulting probabilistic belief on f (using the first and second moments): $m(\mu(x), \Sigma(x, x))$ and $K(\mu(x), \mu(x'), \Sigma(x, x'))$. Approximate the probabilistic belief on f by a GP: $f \sim \mathcal{GP}(m, K)$.
3. Iterate until the budget of evaluations is expended:
 - (a) Select a location to sample next x^* and observe $g(x^*)$. For example, this could be done using uncertainty sampling, which selects the point maximizing the posterior variance of f : $x^* = \arg \max_x K_D(x, x)$
 - (b) Update the posterior belief $g \sim \mathcal{GP}(\mu_D, \Sigma_D)$, fitting the hyperparameters associated with the GP on g by maximizing the marginal likelihood of the observations of f , using the approximate GP belief on f .
4. Calculate the belief about Z given all observations D :

$$Z \sim \mathcal{N}(L[m_D], L^2[K_D]). \quad (2)$$

How to choose the warping function ξ is an open question: clearly ξ must be invertible, but for most constraints that can

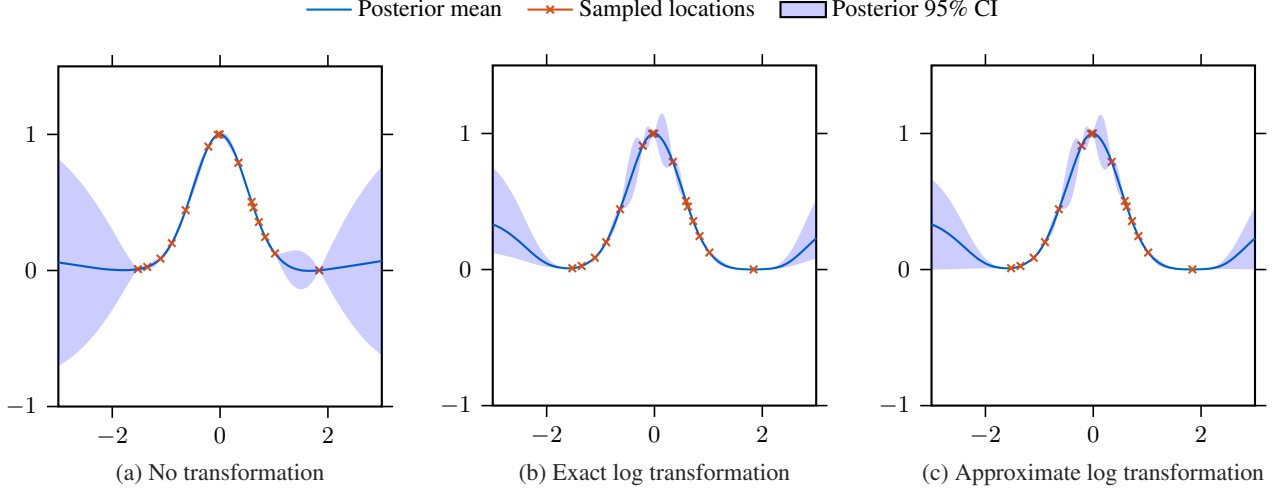


Figure 1: Posterior beliefs, represented using means and 95% credible intervals (CI), on $\exp(-2x^2)$. These plots were generated using a dataset x_D of 15 points sampled uniformly at random from $[-2, 2]$. (a) shows the posterior GP that results from placing a GP prior on f , (b) shows the posterior distribution of the exact log-normal process, i.e., the belief on f if a GP prior is placed on $g = \log f$ and conditioned on x_D and (c) shows a GP posterior with the same first and second moments as the exact log-normal process. All GP priors were parametrized by a constant mean function and a Matérn covariance with $\nu = 3/2$.

be described as a warping of \mathbb{R} , there will generally be multiple choices. This choice may also be affected by the target functional L and the unknown function f . WSABI is clearly an instantiation of this framework with $\xi(x) = \alpha + x^2/2$ and $L[f] = \int f(x)\pi(x) dx$. In Section 4.1, we show that for integrands with a wide dynamic range, our proposed instantiation that uses $\xi(x) = \exp x$ can outperform WSABI.

While the focus of this work will be on quadrature with non-negative functions, note that the above framework is much more general than just this single inference task. As an example of an entirely unrelated task, consider the problem of inferring the gradient of a black box function known to be globally bounded both above and below. Having a probabilistic belief about the gradient of the function can be useful for tasks such as finding global minima and maxima. One possible instantiation of this framework to tackle this inference problem would be to use $\xi(x) = \ell + u/\exp(-x)+1$ (a scaled, logistic function where ℓ and u are the bounds on the objective function) and $L[f] = df/dx$.

3.1. A Moment-Matched Approximation for the Log Transformation

Previous work has been done on using the log transformation for quadrature (Osborne et al., 2012). However, Osborne et al. (2012) only derived a linearized approximation for the posterior GP on f . We present the moment-matched approximation: let $g(x) = \log f(x)$ so that $f(x) = \exp g(x)$. After observing $D = \{x_D, g(x_D)\}$, let $g \sim \mathcal{GP}(\mu_D(x), \Sigma_D(x, x'))$. The mean and variance of

the true posterior on f , a (confusingly named) log-normal distribution, are:

$$m_D(x) = \exp(\mu_D(x) + 1/2\Sigma_D(x, x)); \quad (3)$$

$$K_D(x, x') = m_D(x)(\exp(\Sigma_D(x, x')) - 1)m_D(x'). \quad (4)$$

Figure 1 shows the effect of using the log transformation and the subsequent approximation on the posterior belief using a toy target function, $f(x) = \exp(-2x^2)$. This function is non-negative everywhere so the log transformation is an appropriate choice.

Figure 1(a) shows that placing a GP prior directly on f results in a posterior distribution that does a good job of fitting the data in the region from which samples were drawn. However, there is a great deal of posterior mass below zero, particularly in the unsampled regions, which disagrees with the *a priori* knowledge that f is non-negative. Figure 1(b) shows that the exact, log-normal posterior distribution agrees nicely with the non-negativity constraint as there is no mass below zero, even in the unsampled regions. Lastly, Figure 1(c) shows that the moment-matched GP approximates the exact, log-normal posterior well in the region where samples were drawn from but has a slightly wider variance in the unsampled regions. The approximate posterior also does a good job of imposing the non-negativity constraint on the posterior belief, although because the approximation is a GP, there is necessarily a small amount of mass below zero. Note that this approximation is only necessary to exploit the fact that GPs are closed under affine transformations. If one is performing inference directly

on f , such an approximation is unnecessary and the exact posterior can be used instead.

3.2. Hyperparameter Optimization

Whenever an inference method uses GPs, an important consideration is how to set the associated hyperparameters. One commonly used method is to optimize the marginal likelihood of the observed data using gradient-based methods as the gradient of the marginal likelihood w.r.t. the hyperparameters of the GP is readily available.

The motivation for fitting hyperparameters by maximizing the marginal likelihood is to best explain the observed data. However, when performing inference using the above framework, the goal is not to have the best possible explanation of the transformed data but rather to have an accurate belief about the original, untransformed data. This can be achieved by setting the hyperparameters so as to maximize the marginal likelihood of the untransformed data using the (approximate) posterior belief on f ; optimizing the hyperparameters in this manner will henceforth be referred to as “fitting in f -space” as opposed to “fitting in g -space”.

Formally, if $g \sim \mathcal{GP}(\mu(\theta), \Sigma(\theta))$ (where the dependence on a set of hyperparameters θ has been written out explicitly), then the framework above approximates f as

$$f \sim \mathcal{GP}\left(m(\mu(\theta), \Sigma(\theta)), K(\mu(\theta), \Sigma(\theta))\right),$$

where the exact relationship between θ and the mean and covariance of f depends on the transformation ξ . For many choices of ξ the partial derivatives $\partial m / \partial \mu$, $\partial m / \partial \Sigma$, $\partial K / \partial \mu$ and $\partial K / \partial \Sigma$ will exist everywhere (certainly this is the case for the square root and log transformations, although an interesting line of inquiry would be to formally specify a class of transformations for which this holds). Thus, the partial derivative of f w.r.t. to θ will exist everywhere and the same gradient-based methods used to fit hyperparameters in g -space can be employed to fit hyperparameters in f -space.

Figure 2 shows the result of fitting the hyperparameters in f -space as opposed to fitting the hyperparameters in g -space, again using the toy function $f(x) = \exp(-2x^2)$. Figures 2(a) and 2(c) show that the hyperparameters learned in f -space result in a model that fits the f -space data well but does a very poor job of explaining the data in g -space; the learned mean is much higher than the mean of the transformed data and the learned output scale is very small, leading to unreasonably little uncertainty in the model. However, these learned hyperparameters make sense in the context of the f -space data where most of the observations are functionally zero and the maximum observed value is slightly less than one. Conversely, Figures 2(b) and 2(d) show that the hyperparameters learned in g -space fit the g -space data very cleanly, with a well-scaled uncertainty. However, this

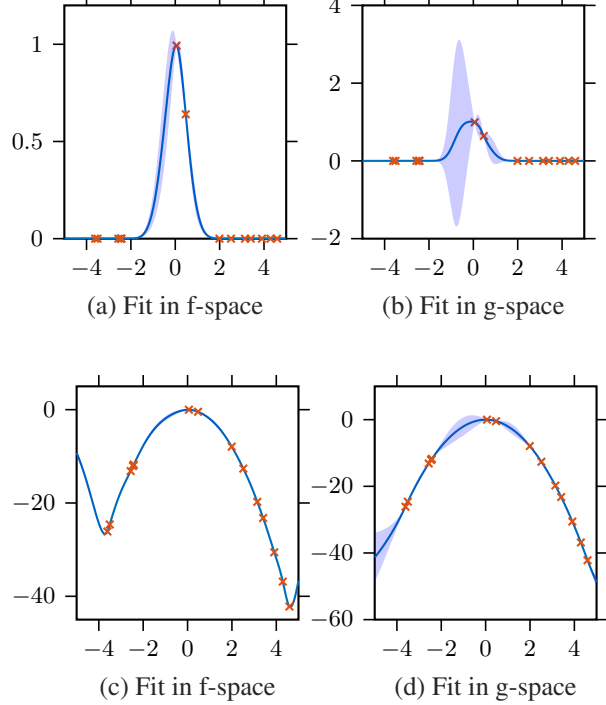


Figure 2: The affect of fitting in f -space vs. fitting in g -space using $f(x) = \exp(-2x^2)$. The plots above were generated by sampling a dataset x_D of 15 points uniformly at random from $[-5, 5]$ and then placing a GP prior on $g = \log f$, parametrized by a constant mean and Matérn covariance with $\nu = 3/2$. This prior has three hyperparameters: a mean, an output scale and a length scale; these hyperparameters were fit in both f -space ((a) and (c)) and g -space ((b) and (d)) to arrive at the plotted posterior beliefs.

translates to a poorly-behaved model in f -space; in particular, the region from $[-2, -0]$ has what appears to be a very reasonable variance in g -space but this corresponds to a massive variance in f -space that strongly defies the non-negativity constraint.

Another interesting metric to compare these two hyperparameter optimization methods on is the probability of the true value of the integral under their respective posterior beliefs on Z . In this case, the true value of the integral can be calculated in terms of error functions: $Z^* = \int_{-5}^5 \exp(-2x^2) dx \approx 1.25$. Given this, the log likelihood of Z^* under the posterior belief arrived at by fitting in f -space is 3.93 vs. 1.48 when fitting in g -space. This difference is because the posterior variance about Z when fitting in g -space is large as a result of the large uncertainty (in f -space) about the function’s value in the region from $[-2, -0]$.

We offer two practical notes about fitting in f -space in the case of a log transform learned through our experiments. First, we suggest shifting the g -space data so that the maximum observed value is exactly zero as this places the ob-

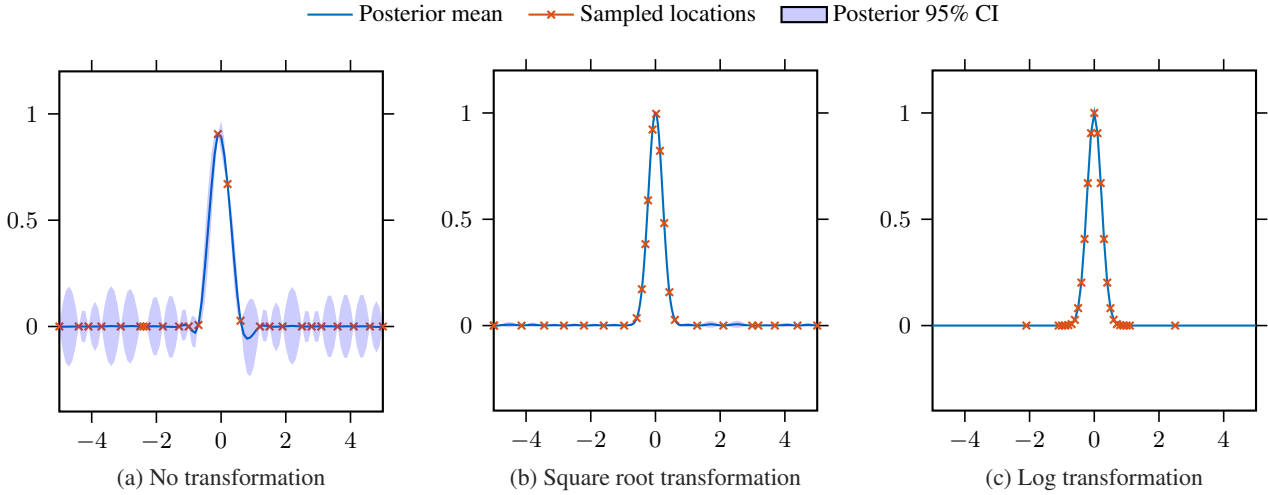


Figure 3: Posterior beliefs of different BQ algorithms on $f(x) = \exp(-10x^2)$ after running for 25 iterations. The target integral was $Z(5, 10) = \int_{-5}^5 \exp(-10x^2/2)^{1/10} dx$. (a) shows the posterior belief of SBQ, (b) shows the posterior belief of WSABI and (c) shows the posterior belief of our method, MMLT. All methods were given the same initial sample, drawn uniformly at random from $[-5, 5]$.

servations into a regime where the inverse transformation is well behaved. We are free to make such a shift when using the log transform as doing so merely equates to multiplying the f -space data by a constant. Second, if one is using a constant mean, we recommend using multiple initializations of the mean and output scale hyperparameters each time the hyperparameters are optimized: in our experiments, each time we fit hyperparameters in f -space, we initialized the mean to $-1, -2, -5, -10$, and -20 and initialized the output scale to the mean initialization divided by -2 . We believe this set of initializations to be sufficient after shifting the data because the relevant portions of the f -space data should be well-described by a hyperparameter setting reachable from one of these initializations; indeed, initializations with lower means may result in undesirable behavior as the corresponding output scales would need to be large (so as to explain the shifted observation at zero), leading to a situation similar to Figure 2(b).

3.3. Approximating the Posterior on Z

For some combinations of linear functionals and warping functions, the posterior belief on Z , as given by equation 2, may be intractable, i.e., either $L[m_D]$ or $L^2[K_D]$ cannot be expressed in closed form. This is the case for quadrature with the log transformation and most common choices of covariance function, including the Matérn and squared exponential (SE) kernels, as the posterior belief contains a term of the form $\int \exp \exp x dx$.

Various approximation techniques can be used to estimate these intractable quantities; in some of the experiments in

Section 4, exhaustive quasi-Monte Carlo (QMC) sampling is used. However, a potentially more-satisfying (at least mathematically) approximation scheme is also explored: using a Taylor series expansion to approximate $m_D(x)$ and $K_D(x, x')$. The exact nature of the Taylor series will depend on the warping function ξ (indeed, for poorly specified ξ , this approximation method may not be available as it requires that $m(\mu, \Sigma)$ and $K(\mu, \Sigma)$ be differentiable w.r.t. μ and Σ): for $\xi(x) = \exp x$, the following approximations follow from equations 3 and 4:

$$m_D(x) \approx 1 + \mu_D(x) + 1/2\Sigma_D(x, x) + (\mu_D(x) + 1/2\Sigma_D(x, x))^2/2 + \dots \quad (5)$$

$$K_D(x, x') \approx 1 + \Sigma_D(x, x') + \Sigma_D(x, x')^2/2 + \Sigma_D(x, x')(\mu_D(x') + 1/2\Sigma_D(x', x')) + \mu_D(x) + 1/2\Sigma_D(x, x)) + \dots \quad (6)$$

Given these approximations, the terms $L[m_D]$ and $L^2[K_D]$ are tractable for certain choices of covariance function, including the SE kernel and all kernels that factorize into independent components along dimensions, i.e., $K(x, x') = \prod_{j=1}^d K_j(x_j, x'_j)$ (Hennig & Garnett, 2016). Unfortunately, computing this approximation is expensive for higher-order terms: computing the i th order term in the Taylor series expansion of either $m_D(x)$ or $K_D(x, x')$ after making n function evaluations takes $\Theta(n^{2i})$ time. However, we will see that for the log transform employed here, even a first-order approximation performs well.

4. Experiments

In this section, we run multiple experiments using our proposed algorithm for Bayesian quadrature using a moment-matched log transformation (MMLT) and compare the results against WSABI and SBQ as well as Monte Carlo methods. If not otherwise specified, all GP priors were chosen to have constant mean and Matérn covariance with $\nu = 3/2$, all sample locations were selected iteratively using uncertainty sampling in f -space, all hyperparameters were fit in f -space when applicable, and all intractable posteriors were estimated using exhaustive QMC sampling.

4.1. Synthetic Data

We consider estimating

$$Z(a, C) = \int_{-a}^a \exp(-Cx^2/2) \frac{1}{2a} dx$$

(an unnormalized Gaussian likelihood against a uniform prior). Figure 3 shows the posterior GPs of MMLT (Figure 3(c)), WSABI (Figure 3(b)) and SBQ (Figure 3(a)) on $f(x) = \exp(-10x^2/2)$ after 25 samples while estimating $Z(5, 10)$. The posterior belief of SBQ has a great deal of mass below zero, mostly because the learned length scale is short in order to account for the speed at which the function goes from one to zero. WSABI's posterior is better at imposing the non-negativity constraint but the nearly uniform distribution of samples over the domain indicates that WSABI was unable to clamp down its uncertainty as efficiently as MMLT. Thus, uncertainty sampling led WSABI to sample in regions that contribute effectively zero mass to the integral. MMLT, in addition to having a posterior belief that has very little mass below zero, has the highest sample efficiency, clustering its samples in the most informative regions: where the function transitions from having zero mass to having some mass.

Taking C to be a proxy for the dynamic range of the integrand, Figure 4 shows the effect that increasing dynamic range has on the accuracy of each method; in order to evaluate each method's accuracy, the true values of all $Z(5, C)$ were calculated using error functions as in Section 3.2. Although both SBQ and WSABI are competitive with MMLT at lower values of C , as the dynamic range of the integrand increases, MMLT's accuracy stays high whereas the performance of both SBQ and WSABI fall off, with SBQ's performance falling off rapidly.

4.2. Detecting DLAs via Model Selection

Our real-world application is a model selection problem from astrophysics: predicting whether a damped Lyman- α absorber (DLA) exists on the sightline between a quasar and earth. DLAs are large gaseous clouds containing neutral hydrogen at high densities. Their location and size can be

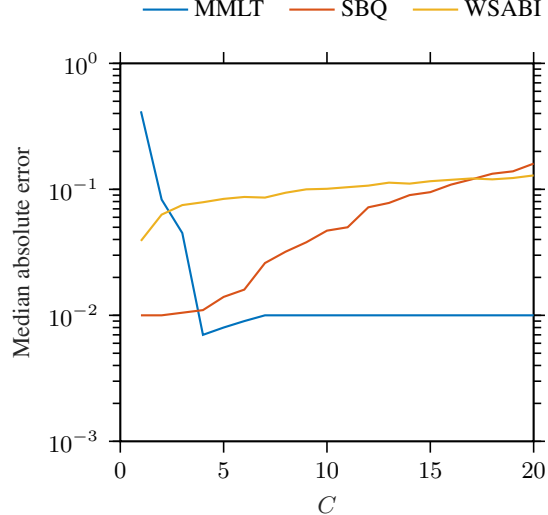


Figure 4: Accuracy of MMLT, WSABI and SBQ. This plot was generated by using each BQ algorithms to estimate $Z(5, C)$ for $C \in \{1, \dots, 20\}$. Each algorithm was run 100 times for 25 iterations. For each run, the initial sample was drawn uniformly at random from $[-5, 5]$. The median absolute error of each method's estimate of the log of the integral at termination is plotted above.

inferred from observations of quasar spectra as they cause distinctive dips in the observed flux at well-defined wavelengths of radiation. Astrophysicists are interested in detecting DLAs as they give insight into the history of galaxy formation. Garnett et al. (2017) developed a model that specifies the likelihood that a given emission spectrum contains a DLA. The model is parameterized by two physical features of a candidate DLA: its column density, which roughly corresponds to its size, and its redshift, which roughly corresponds to its distance from earth. Garnett et al. (2017) also specified a data-driven prior distribution over these two parameters, which must be integrated against to calculate the model evidence. Thus, the model evidence for the existence of a DLA is an (intractable) integral over the domain (as defined by the prior) of these two model parameters. For a complete description of the problem and model, see (Garnett et al., 2017).

Figure 5 contains a sample log-likelihood surface as a function of the model's two parameters: note that the surface is highly multimodal, with the peaks occurring at low column densities, and that the dynamic range of the function is massive, ranging from around -1000 to around -25 000 in log space. These features make computing the model evidence a difficult task for SBQ and WSABI. Although the model evidence for the existence of a single DLA is a 2-dimensional integral, the number of dimensions can be scaled up to any even number simply by calculating the model evidence for the existence of n DLAs, resulting in a $2n$ -dimensional integral.

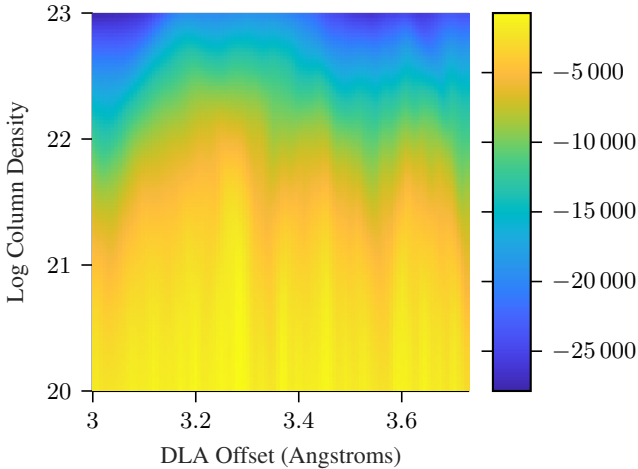


Figure 5: The log-likelihood of a candidate DLA, defined by its log column density and its redshift, for a sample quasar emission spectrum (not pictured) generated using the model developed by Garnett et al. (2017). This spectrum is known to contain a DLA at redshift 3.28 with a log column density of 20.39.

Figure 6 shows results of our experiments run on 2- and 6-dimensional integrals. We compare MMLT’s accuracy at estimating these integrals against WSABI and SBQ as well as sequential Monte Carlo and QMC, drawing samples from the prior specified by Garnett et al. (2017) and a scrambled Halton sequence (Kocis & Whiten, 1997) respectively. We show the median absolute error over time as the comparison is between the logs of the quadrature methods’ estimates and the true model evidence. MMLT outperforms all other methods except for QMC on both of these experiments; note that in general, QMC is not well-suited for model-selection problems due to the inability to build an appropriate low-discrepancy sequence, and we use it here to provide a gold-standard baseline. The difference in absolute errors at termination between MMLT and both other BQ methods is significant for the 6-dimensional integrals but not for the 2-dimensional integrals at a 1% significance level according to a one-sided paired t-test

Table 1 compares the three BQ methods on the metric introduced in Section 3.2: the log-likelihood of the “true” value of the integral Z^* under each method’s posterior belief upon termination. MMLT significantly outperforms the other Bayesian algorithms on this metric in both the 2-dimensional and 6-dimensional experiments, again at a 1% significance level according to a one-sided paired t-test.

4.2.1. HYPERPARAMETER OPTIMIZATION EXPERIMENTS

To investigate the effect of our proposed hyperparameter optimization methodology, we compared fitting hyperparameters in f -space against fitting them in g -space in the

Table 1: Mean $\log p\{Z^* | D\}$ at termination. The values in the table below were generated by running the three BQ methods on 2000 2- and 6-dimensional model evidences for 5 and 60 seconds respectively and then calculating the average log-likelihood of the “true” model evidence under each BQ method’s posterior distribution over the model evidence upon termination.

DIMENSION	MMLT	WSABI	SBQ
2	11.1	4.40	4.19
6	1.93	-0.557	0.773

DLA model evidence setting on two metrics: the median log-likelihood of the “true” (2-dimensional) model evidences under the posterior beliefs, $\log p\{Z^* | D\}$, and the mean expected predictive probability, $\mathbb{E}[p\{f(x) | x, D\}]$, $x \notin D$. The latter metric was estimated by averaging over the predictive probabilities of the QMC samples used to estimate the model evidence.

Table 2: Fitting in f -space vs. fitting in g -space. To generate the values below, we randomly sampled 20 sets of 100 samples from the prior for each of the 2000 spectra, giving a total of 40 000 data sets. Each data set was used to optimize the hyperparameters of a GP prior on the log of the integrand in both f -space and g -space.

METHOD	$\log p\{Z D\}$	$\mathbb{E}[p\{f(x) x, D\}]$
FIT IN F-SPACE	0.614	7.24
FIT IN G-SPACE	-161 000	0.0693

As Table 2 shows, fitting in f -space outperforms fitting in g -space in both categories by orders of magnitude. The relatively poor performance of fitting in g -space on both metrics is largely because the high dynamic range of these likelihood surfaces forces the learned output scale (in g -space) to be high. This in turn causes both the pointwise distributions and the distribution on the value of the integral to have large variances (relative to their means), thus making the likelihood everywhere low.

4.2.2. TAYLOR SERIES EXPERIMENTS

We analyzed the ability of a Taylor series to approximate the intractable posterior mean that arises in MMLT. Table 3 shows the accuracy of different Taylor series approximations when compared with an exhaustive QMC approximation.

The Taylor series estimates approximate the QMC estimate well, particularly when using factorized Matérn kernel. Note that the fractional errors for the 6-dimensional integrals are lower across the board than the 2-dimensional fractional errors, indicating that the Taylor series approximations are relatively closer in value to the QMC estimates of the posterior means for these integrals. We hypothesize this to be the case because in the higher dimensional space, the samples cover a smaller percentage of the total volume and the

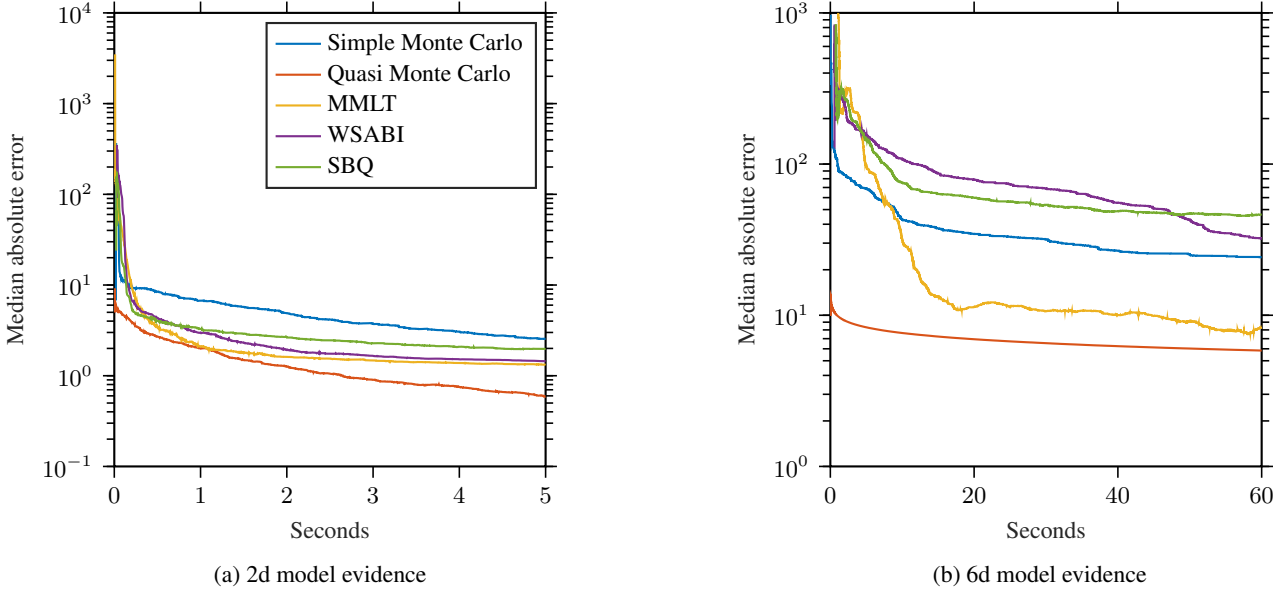


Figure 6: DLA experiments. Each of the three BQ algorithms was used to estimate the model evidence for a single DLA and three DLAs in a set of 2000 quasar emission spectra, resulting in 2- and 6-dimensional integrals. We also compared against sequential variants of Monte Carlo and quasi-Monte Carlo estimates. Each quadrature method was allotted 5 seconds for the 2-dimensional integrals and 60 seconds for the 6-dimensional integrals. The median absolute error of each method’s estimate of the log model evidence over time is plotted above; the “true” value of the log model evidence was calculated using exhaustive QMC sampling.

Table 3: Median fractional errors of Taylor series approximations. Using both a SE kernel with automatic relevance determination and a factorized Matérn kernel with $\nu = 3/2$, we ran MMLT for 100 iterations on 2000 2-dimensional model evidences and for 200 iterations on 500 6-dimensional model evidences. We estimated the posterior mean of MMLT’s belief about the model evidences using both first- and second-order Taylor series expansions.

DIMENSION	FIRST-ORDER		SECOND-ORDER	
	SE	MATÉRN	SE	MATÉRN
2	0.0155	0.0036	0.0436	0.0149
6	0.0015	0.0017	0.0012	0.0014

unsampled regions under the posterior belief are well represented by a low-order approximation. Furthermore, observe that a first-order approximation appears to be sufficient for estimating this quantity, despite the fact that the posterior mean is of the highly nonlinear form $\exp f(x)$. This is a convenient byproduct of subtracting the maximum observed value from all observations (see Section 3.2), as this loosely upper bounds the exponent of the posterior mean at zero, a region of the function that is particularly well behaved.

5. Conclusion

In this work, we have presented a general, Bayesian framework for performing inference on constrained functions. As a part of this framework, we developed a novel proce-

dure for optimizing the hyperparameters associated with our framework whereby the hyperparameters are set to maximize the marginal likelihood of the true data as opposed to maximizing the marginal likelihood of the transformed data. Although maximizing the marginal likelihood of the transformed data may seem intuitive as that directly corresponds to the function on which a GP prior is placed, we show that doing so can lead to undesirable behavior, particularly if the target function has a wide dynamic range.

We also developed an instantiation of our proposed framework for performing quadrature on non-negative functions using the log transformation. We show that this novel BQ algorithm outperforms previously offered BQ algorithms on synthetic and real-world data, both in terms of accuracy and speed of convergence.

In future work, we hope to extend this framework to other inference tasks, such as the one mentioned in Section 3. Also, we hope to augment this framework to be able to incorporate the observation of not just function values but other linear functionals of the target function (e.g., gradients) as GPs are closed under conditioning on any linear functionals. While the effect of incorporating gradient observations has been studied in other inference tasks such as Bayesian optimization (Jones et al., 1998; Wu et al., 2017), to the best of our knowledge the impact of including gradients into a quadrature algorithm has never been explored.

References

Diaconis, Persi. Bayesian numerical analysis. *Statistical Decision Theory and Related Topics*, 4(1):163–175, 1988.

Garnett, Roman, Ho, Shirley, Bird, Simeon, and Schneider, Jeff. Detecting Damped Lyman- α Absorbers with Gaussian Processes. *Journal of Statistical Planning and Inference*, 472(2):1850–1865, 2017.

Gunter, Tom, Osborne, Michael A., Garnett, Roman, Hennig, Philipp, and Roberts, Stephen J. Sampling for Inference in Probabilistic Models with Fast Bayesian Quadrature. *Advances in Neural Information Processing Systems*, 2014.

Hennig, Philipp and Garnett, Roman. Exact Sampling from Determinantal Point Processes. *arXiv preprint arXiv:1609.06840 [cs.LG]*, 2016.

Jones, Donald R., Schonlau, Matthias, and Welch, William J. Efficient Global Optimization of Expensive Black-Box Functions. *Journal of Global Optimization*, 13:455–492, 1998.

Kocis, Ladislav and Whiten, William J. Computational Investigations of Low-Discrepancy Sequences. *ACM Transactions on Mathematical Software*, 23(2):266–294, 1997.

Meng, Xiaoli and Wong, Wing H. Simulating ratios of normalizing constants via a simple identity: a theoretical exploration. *Statistica Sinica*, 6(4):831–860, 1996.

Neal, Radford M. Annealed importance sampling. *Statistics and Computing*, 11(2):125–139, 2001.

O’Hagan, Anthony. Bayes-hermite quadrature. *Journal of Statistical Planning and Inference*, 29:245–260, 1991.

Osborne, Michael A., Garnett, Roman, Ghahramani, Zoubin, Duvenaud, David, Roberts, Stephen J., and Rasmussen, Carl E. Active learning of model evidence using Bayesian quadrature. *Advances in Neural Information Processing Systems*, 2012.

Rasmussen, Carl E. and Ghahramani, Zoubin. Bayesian Monte Carlo. *Advances in Neural Information Processing Systems*, 2003.

Rasmussen, Carl E. and Williams, Christopher K.I. *Gaussian Processes for Machine Learning*. MIT Press, 2006.

Skilling, John. Nested sampling. *Bayesian inference and maximum entropy methods in science and engineering*, 735:395–405, 2004.

Wu, Jian, Poloczek, Matthias, Wilson, Andrew Gordon, and Frazier, Peter I. Bayesian Optimization with Gradients. *Advances in Neural Information Processing Systems*, 2017.